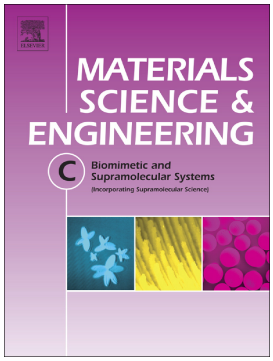

Fabrication and investigation of a biocompatible microfilament with high mechanical performance based on regenerated bacterial cellulose and bacterial cellulose

Huan-ling Wu, David H. Bremner, Hai-jun Wang, Jun-zi Wu, He-yu Li, Jian-rong Wu, Shi-wei Niu, Li-min Zhu

PII: S0928-4931(17)30676-8
DOI: doi: 10.1016/j.msec.2017.05.073
Reference: MSC 8055

To appear in: *Materials Science & Engineering C*

Received date: 20 February 2017
Revised date: 5 May 2017
Accepted date: 13 May 2017

Please cite this article as: Huan-ling Wu, David H. Bremner, Hai-jun Wang, Jun-zi Wu, He-yu Li, Jian-rong Wu, Shi-wei Niu, Li-min Zhu , Fabrication and investigation of a biocompatible microfilament with high mechanical performance based on regenerated bacterial cellulose and bacterial cellulose, *Materials Science & Engineering C* (2017), doi: 10.1016/j.msec.2017.05.073

Fabrication and investigation of a biocompatible microfilament with high mechanical performance based on regenerated bacterial cellulose and bacterial cellulose

Huan-ling Wu [a,b], David H Bremner [c], Hai-jun Wang [a], Jun-zi Wu [a], He-yu Li [a], Jian-rong Wu [a], Shi-wei Niu [a], Li-min Zhu [a,*]

[a] College of Chemistry, Chemical Engineering and Biotechnology, Donghua University, Shanghai 201620, P. R. China

[b] Jiuzhou College of Pharmacy, Yancheng Institute of Industry Technology, Yancheng 224005, P. R. China

[c] School of Science, Engineering and Technology, Kydd Building, Abertay University, Dundee DD1 1HG, Scotland, UK

***Corresponding author:**

Prof. Li-Min Zhu, Ph.D,

College of Chemistry, Chemical Engineering and Biotechnology,

Donghua University,

2999 North Renmin Road, Songjiang District,

Shanghai 201620, China,

Tel: +86-21-67792748,

Fax: +86-21-62372655,

E-mail: lzhu@dhu.edu.cn

ABSTRACT： A high-strength regenerated bacterial cellulose (RBC)/bacterial cellulose (BC) microfilament of potential use as a biomaterial was successfully prepared via a wet spinning process. The BC not only consists of a 3-D network composed of nanofibers with a diameter of several hundred nanometers but also has a secondary structure consisting of highly oriented nanofibrils with a diameter ranging from a few nanometers to tens of nanometers which explains the reason for the high mechanical strength of BC. Furthermore, a strategy of partially dissolving BC was used and this greatly enhanced the mechanical performance of spun filament and a method called post-treatment was utilized to remove residual solvents from the RBC/BC filaments. A comparison of structure, properties, as well as cytocompatibility between BC nanofibers and RBC/BC microfilaments was achieved using morphology, mechanical properties, X-ray Diffraction (XRD) and an enzymatic hydrolysis assay. The RBC/BC microfilament has a uniform groove structure with a diameter of 50~60 μm and XRD indicated that the crystal form was transformed from cellulose Iα to cellulose III_I and the degree of crystallinity of RBC/BC (33.22%) was much lower than the original BC (60.29%). The enzymatic hydrolysis assay proved that the RBC/BC material was more easily degraded than BC. ICP detection indicated that the residual amount of lithium was 0.07 mg/g (w/w) and GC-MS analysis showed the residual amount of DMAc to be 8.51 μg/g (w/w) demonstrating that the post-treatment process is necessary and effective for removal of residual materials from the RBC/BC microfilaments. Also, a cell viability assay demonstrated that after post-treatment the RBC/BC filaments had good cytocompatibility.

Keywords: Nanofibril bundles; Regenerated bacterial cellulose; Biomedical materials; Residual solvent; Cytocompatibility

1. Introduction

Bacterial cellulose (BC) is a biomass, synthesized by bacteria and has the same molecular structure as plant cellulose, and both are composed of polysaccharides with linear chains of β-1,4-D glucopyranose residues. The manufacturing process of BC is economical and environmentally friendly and BC exhibits outstanding properties and is one of the most abundant renewable organic materials on earth [1]. Due to its advantages in structure, performance, ease of production and application, BC is superior to plant cellulose [2] and has shown good promise in the field of biomaterials [3-7]. However, natural BC lacks structural diversity, so it is necessary to modify it in order to enlarge its field of potential applications.

BC can be converted into cellulose derivatives (ethers and esters) and regenerated bacterial cellulose (RBC) materials (membranes, fibers, food casings, sponges, etc.) [8]. In the current work, a wet spinning regeneration process was investigated since it has superior performance with regard to material, equipment and parameters compared to wet filming (casting film using BC solution) and there are a few reports of the preparation of RBC filaments from BC solution in the literature. Previous research on RBC mainly focused on the preparation of RBC film not fibers/filaments [9]. In industry, it is necessary for some materials to be processed in the form of fibers/filaments since the yarns or filaments made from wet spinning fibers can be further converted into non-woven, woven and knitted fabrics or sutures that can be used in medical or other areas [10,11]. As previously described [12,13], wet spinning technology is suitable for the preparation of such materials where the melting temperature is higher than its degradation temperature and BC fits into this category. To date, there have been few theoretical or experimental studies on RBC filaments prepared by wet spinning so consequently research on this issue is considered to be of considerable importance and timely.

The use of an appropriate solvent which will dissolve BC into a spinning solution with a certain viscosity and rheological behavior is the premise of wet spinning. Recent reports have mainly focused on finding a good solvent, such as NaOH/urea solution [9], N-methylmorpholine-N-oxide monohydrate (NMMO) [14,15], ionic liquids [16,17], N,N-dimethylacetamide (DMAc)/lithium chloride (LiCl) [18,19] or $ZnCl_2$ [20] for the BC. Among these, the use of DMAc/LiCl in the dissolving process is the most common due to ease of operation, low cost and being less energy demanding. Thus, this paper describes the preparation, via a wet spinning process, and properties of an RBC/BC microfilament for potential use as a biomedical material. The main objective of this study was to use BC as the raw material, LiCl/DMAc as the solvent system and DMAc/water as the coagulation bath in order to improve the wet spun filaments by controlling the swelling and dissolution time of BC to enhance the mechanical strength (Fig. 1). BC has an ultra-fine fibrous 3-D network structure with high purity, high mechanical strength, wet capability and good biocompatibility [21]. In the current work, the nature of the BC was partially conserved during the dissolving process ensuring that its excellent properties, especially the high mechanical strength, was maintained and enhanced in the resulting RBC/BC microfilament. The rheological morphological, mechanical properties, X-ray Diffraction (XRD) as well as the enzymatic hydrolysis performances were all studied in order to determine the differences between the BC fiber membrane and RBC/BC filaments with respect to structure and properties.

Fig. 1

An ideal biomaterial must provide a variety of shapes and sizes, be biocompatible, absorbable and capable of being replaced by new tissue formation, in the case of applications in tissue engineering. Currently, natural polymers

are important alternatives as scaffolds for tissue repair [22] and over the past decade, types of materials based BC have been designed for a diversity of biomedical applications. Previous work in this area concentrated on BC or BC composites rather than RBC and no relevant study on the issue of residual solvent/ions produced during the process of BC regeneration has been reported. Residual solvents (RS) and residual ions (RI) may represent a potential risk for human health due to their toxicity and their undesirable side effects [23] and they should be removed through some form of effective post-treatment. Hence, for the first time, an attempt was made to detect RS in RBC filaments using gas chromatography-mass spectrometry (GC-MS) and Inductively Coupled Plasma Emission Spectrometry (ICP-MS) was utilizes to measure the amount of RI. A cytocompatibility assay test was performed to examine the differences of cell (L929 cells) viability between the RBC/BC filaments with and without post-treatment. Moreover, in this work, not only is the preparation of a RBC/BC microfilament, with high mechanical performance, described but also data is given to provide for its better future application through a comprehensive analysis of the properties of the BC before and after regeneration.

2. Materials and methods

2.1. Materials

Bacterial cellulose was provided by Hainan Yida Co., Ltd. (Guangdong, China). Cellulase from Aspergillus niger (product #C0057, 10 000 U/g, slightly brown powder) was purchased from Okyo Chemical Industry (TCI). The following chemicals were purchased from Sinopharm Chemical Reagent Co., Ltd: dimethylacetamide (DMAc, ≥ 99%), lithium chloride (LiCl, ≥97%), sulfuric acid (≥98%), Avicel citric acid (≥99.5%), sodium citrate dihydrate (meets USP testing specifications), 3,5-dinitrosalicylic acid (DNS, ≥98%), ethyl alcohol (EtOH, ≥99%), acetone (≥

99%).

2.2. Dissolution and regeneration of BC

The preparation of spinning dope was carried out as follows: firstly, wet BC membrane was cut into small pieces and crushed by a high speed homogenizer at 15,000 rpm for 30 min to form a BC slurry which was freeze-dried at −40 ℃ for 2 days. Secondly, a DMAc/ LiCl (7% - 8% w/w) mixed solvent was prepared and the dried BC slurry (3.0 g) was suspended in DMAc/ LiCl (147.0 g). This superior dispersion system was stirred with mechanical agitation (50 - 60 r/ min) for a certain time (6, 8, 10, 12, 14, 16, 18h) at room temperature until virtually all the BC dissolved and then a RBC/BC spinning solution (2%, w/w) was prepared as described in the supplementary documents (Fig. S1).

The method of recasting RBC film has been reported in the literature [15,19] and was utilized in this work. The solution prepared above was poured into a culture dish with a diameter of 60 mm and then coagulated in a DMAc/water solution (500mL; 30:70v/v) for 5 min. After freeze-drying at −40 ℃ for 2 days, a RBC film with a thickness of 0.1 mm was produced.

RBC/BC microfilaments were spun on a custom-made wet-spinning device (Fig. S2), which has been described previously, using the spinning process parameters shown in Table S1. A nitrogen pressure of 0–0.3 MPa was used to extrude the aqueous solutions (2% w/w) at 1.0 mL/min through a commercial spinneret plate with a single 0.25 mm diameter orifice. The spinning dope was extruded directly into an aqueous DMAc/water (50% v/v) coagulant solution kept below 15 ℃. The total length of the coagulation bath, the second bath and the third bath was 60 cm and after passing though these baths and over the three rollers, the resulting microfilaments were wound onto spools and dried at room temperature for 2 h. The appearance of prepared RBC/BC filaments in the dry state and wet state

are also shown in Fig. S2. Further, it is necessary to use a strategy called post-treatment process whereby the filament samples are soaked in Millipore hot water (≥60℃) for 30 min, then centrifuged at 2500 rpm at 20°C for 5 min. This process was repeated once more in order to remove as much residual solvent and ions as possible.

2.3. Optical microscope (OM) analysis

The optical imaging was performed using a custom-modified BX-51 Olympus optical microscope equipped with a color digital CCD camera (Lumenera Infinity 2−1C). Various diluted samples (50 μL) of the RBC/BC solution were spread on a glass slide and then observed by OM.

2.4. Mechanical properties

The single filament fineness was measured using the middle section cutting method. The mechanical properties of single microfilaments were measured with a XQ-2 Fiber Tension Meter (Shanghai S&CI, Shanghai, China) using a filament holder of 20 mm in length and a crosshead speed of 20 mm/min. All samples were preconditioned at 20 °C and 65% relative humidity for 24 h prior to mechanical testing and the breaking strength and elongation at break of the RBC/BC filaments were calculated and the mean and standard deviation reported for n = 20.

2.5. Transmission electron microscope (TEM) analysis

TEM imaging of the hyperfine structure of BC was conducted on a JEM-2100 (Japanese Electronics Co. Ltd，Japan) by drop casting the sample onto a carbon-Formvar TEM grid. To minimize radiation damage and to use the smallest objective aperture for enhancing contrast, measurements were operated at 80 kV acceleration voltage.

The TEM samples were prepared using the referenced method for cellulose nanocrystals (CNCs) as described [24,25] but using different parameters. Briefly, the freeze-dried BC fragments (1g) were hydrolyzed in 50 mL sulfuric acid solution at a concentration of 60% (w/w) at 35 ℃ with vigorous stirring for 45 min. The cellulose

suspension was then diluted with cold Millipore water to stop the hydrolysis reaction. The remaining white suspension was centrifuged at 8000 rpm at 4 ℃ for 10 min to collect the hydrolyzed products which was then dialyzed with regenerated cellulose dialysis tubing (12 000-14 000 MWCO, Thermal Scientific) against Nanopure water until the pH reached a constant value. Sonication was performed on the aqueous BC nanocrystals using a Branson Sonifier for 30 min at ice bath temperature. The resulting colloidal suspension was centrifuged at 5000 rpm at 4 ℃ for 5 min, and then the cloudy supernatant was collected and stored at 4 ℃ prior to use. The sample was diluted to 0.05 mg/mL before TEM testing.

2.6. Rheological measurements

The rheological measurements were performed on ARES-RFS Rotational Rheometer (TA Instruments, USA) using a cone plate with a diameter of 50 mm. The rheological properties of the RBC/BC spinning solution were determined at 25 ℃. In a Newtonian fluid the shear stress is directly proportional to the shear rate but some liquids, such as the spinning solutions under study, are termed non-Newtonian and the degree of deviation (the non-Newtonian index n) may be calculated using Eq. (1):

$$\lg \sigma_\tau = \lg K + n \lg \dot{\gamma} \qquad (1)$$

where σ_τ (Pa) is the shear stress, $\dot{\gamma}$ (S^{-1}) the shear rate and K the viscosity coefficient. The value of the non-Newtonian index (n) is obtained from the slope of the curves after plotting $\lg \sigma_\tau$ versus $\lg \dot{\gamma}$.

2.7. Morphology analysis

The prepared samples were sputtered with gold prior to observation using a JSM-5600LV scanning electron microscope (JEOL, Tokyo, Japan).

2.8. Wide angle X-ray diffraction (XRD) analysis

XRD measurements were performed on very small pieces (ca. ≤ 0.2 mm) of the microfilaments using a wide angle X-ray diffractometer (D/max-2550 PC, Japan). A scanning rate of 0.058 ° s^{-1} was applied to record the pattern in the 2θ range of 10-70°. The operating voltage and current were 40 kV and 200 mA, respectively, using Ni-filtered Cu-Ka radiation of wavelength 0.15406 nm.

2.9. Fourier transform infrared spectroscopy (FT-IR) analysis

The FTIR-ATR spectra of the BC nanofiber membrane and the RBC/BC microfilaments were recorded using a Nicolet-Nexus 6700 FTIR spectrometer (Nicolet Instrument Corp., USA) over the wavenumber range of 500−4000 cm^{-1} at a resolution of 4 cm^{-1}, a scan speed of 0.2 cm/s and 32 scans were recorded per sample.

2.10. Enzymatic hydrolysis

Two enzymatic degradation methods were used to evaluate the differences between the BC and RBC/BC materials and all the experiments were run in triplicate.

Method (1) involved hydrolysis with different enzyme concentrations but keeping the time constant. A series of solutions with different cellulase concentrations (0, 2.0, 5.0, 10.0, 50.0 mg/mL) using citrate buffer solution (50 mM; pH 5.0) as solvent were prepared. Then, the same amount of the untreated BC slurry and RBC/BC filaments (5.0 mg, dry weight) were added into the different concentrations of medium (2.5 mL). The enzymatic degradation was carried out at 50 ℃ under gentle stirring for 2 h and the concentration of reducing sugars were determined.

Method (2) used hydrolysis with the same enzyme concentration but varying the time. Cellulase (100 mg) was suspended in citrate buffer solution (20 mL; 50 mM; pH 5.0) to prepare a cellulase incubation medium (5 mg/mL). The same amount of untreated BC slurry and RBC/BC filaments (5.0 mg, dry weight) in the cellulase medium (5.0

mL) were incubated in a water bath (Jintan Instrument Co. Ltd., Jiangsu, China) at 50 ℃ under gentle stirring. An aliquot (0.5 mL) was removed for sugar analysis at regular intervals and the remaining volume was kept constant by the addition of fresh cellulase medium (0.5 mL). The reducing sugar analysis was performed according to the IUPAC method [26,27].

2.11. Inductive Coupled Plasma Emission Spectrometer (ICP-MS) detection

The samples were first digested with a Multiwave system (SpeedWave Entry, Berghof, Germany) using samples (~0.1 g) suspended in 65 % HNO_3 (5 mL) and 30 % H_2O_2 (1 mL) heated to 200 ℃. The digestion solutions were measured using an Inductive Coupled Plasma Emission Spectrometer (ICP-MS, Prodigy, Leeman Labs, USA).

2.12. Pyrolysis gas chromatography-mass spectrometry (PyGC-MS) using gas chromatographic headspace (HSGC) method

Measurements of activity coefficients at infinite dilution for a set of low polar volatile organic substances were made using headspace analysis technique. Analysis was performed using a Shimadzu GC system (GCMS-QP-2010, Japan) equipped with an oven having temperature programming capability and a flame ionization detector (FID). In the experiment, RBC filaments (100 mg), with and without post-treatment, were placed in glass vials, sealed and thermostated. Samples (n = 2) from the vapor phase after equilibrium were transferred through a heated quartz glass line into the injector of a gas chromatograph. The area of a peak S corresponding to the analyte (DMAc) was calculated. Standard solutions were prepared by diluting appropriate volumes of pure solvent (DMAc) in acetone (1.0, 2.0, 4.0, 8.0 μg/mL) and a standard line was obtained: Eq. (2).

$Y = 541741\ X - 33861$ (2)

$R^2 = 0.9993$

2.13. Cell culture and cytocompatibility assay

L929 cells were selected as a model cell line for the cytocompatibility assay. Three groups of samples, wet spun fibers (3.0 mg, with and without post-treatment) and BC fragments (3.0 mg) were placed in 24-well plates and another group without fabric was set as the control. The culture plates were sterilized by alcohol steam for 4 h and PBS solution was used for washing away any residual alcohol. After being soaked with Dulbecco's Modified Eagle Medium (DMEM), all the culture plates incubated for 24 h (37 °C, 5% CO_2). After this time, a suspension of L929 cells (200 μL; with a cell density of 1.0×10^4 cells/mL) was seeded into each well with DMEM (containing10% FBS) and then incubated (37 °C, 5% CO_2). The time points of the test were set as 1, 3 and 5 days and at each point, the culture plates were taken out of the incubator and the DMEM in every well was replaced by fresh DMEM (360 μL) and MTT (40 μL) solutions. After incubation for 4 h, DMSO (400 μL) was added to each well and the plates shaken for 30 min at room temperature. Afterwards, the solutions in each well were transferred into 96-well plates and the OD values of the resulting purple solutions were measured at 570 nm with a Microplate Reader (Multiskan, ThermoFisher, USA). Mean and standard deviation for the triplicate wells were reported.

After washing twice with PBS (pH 7.4) the cell morphology was observed under a Zeiss inverted fluorescence microscope (200 × magnification, Jena, Germany).

2.14. Statistical analysis

Statistical analysis was carried out using the unpaired Student's t-test on SAS software (version 9.0). A value of $p < 0.05$ was considered statistically significant. Data are annotated with * for $p < 0.05$, ** for $p < 0.01$, and *** for $p < 0.001$.

3. Results and discussion

3.1. Acid-hydrolysis, swelling, and dissolution of BC

An acid-hydrolysis method was performed to prepare bacterial cellulose nanocrystals (BCNCs) to investigate the ultra-fine structure. BC has an obvious 3-D fine structure which can be observed by SEM (Fig. 6a) but, surprisingly, a hyperfine structure consisting of a more elaborate and oriented nanofiber bundle has been found and observed by TEM for the first time (Fig. 2) with the diameters of single ultrafine nanofibrils ranging from a few nanometers to tens of nanometers. This result strongly demonstrates that the high mechanical strength of BC is due to a 3-D network composed of nanofibers with a diameter of several hundred nanometers (Fig. 6a) and also the secondary structure consisting of highly oriented nanofibrils with more smaller diameters.

Fig. 2

A dissolving method using DMAc/LiCl as solvent was used to prepare a spinning solution for wet spinning and swelling of the cellulose fibers is an important step prior to dissolution. When BC is placed in DMAc/LiCl, the solvent initially only penetrate into the semipermeable and elastic areas of the fiber wall when the diffused molecules cause radial expansion of the secondary wall. In the swelling process, Cl^- ions form hydrogen-type interactions with

the hydroxyl group hydrogens of cellulose, breaking the existing bonds in the interior of the structure. Meanwhile, Li^+ ions interact with the carbonyl group oxygen of the DMAc molecule, forming a $[DMAc_n + Li]^+$ chelation structure [28] which acts as a spacer between cellulose chains prohibiting the formation of intermolecular hydrogen bonds. After the BC fibers swell completely, intermolecular bonds are broken finally due to the stress produced by the swelling process. With a very strong solvent, it is possible to disrupt the entire crystalline structure [29] although a short swelling time does not decrease the crystallinity sufficiently but a longer time leads to complete dissolution.

Fig. 3

Based on the discussion above a new process, involving the partial retention of undissolved BC during the preparation of the spinning solution, and which might increase the strength of spun fibers, was investigated. However, the relationship of swelling state and swelling time first needed to be determined. After stirring in DMAc/LiCl for different times the BC solution was observed by OM (Fig. 3) and it is seen that some intact BC skeleton structure still exists after 6 h (Fig. 3a) but only a very small amount remains at 10 h (Fig. 3b). When the stirring time reaches 14 h, a homogeneous BC solution is present (Fig. 3c) but the solution may still contain small amounts of undissolved BC which are invisible which is in agreement with a previous report [29]. Hence, it is concluded that the time for the complete dissolution of BC ranges from 12-16 h.

3.2. The mechanical properties of RBC/BC microfilaments

Mechanical strength is a very important property regarding further use of any material and evaluation of the strength and elasticity of the filaments was determined by breaking strength and elongation tests. As discussed above,

the dissolving time was monitored by viewing the swelling/dissolution of the RBC/BC filaments utilizing optical microscopy (Fig. 3) and the optimal time was found to be around 14 h where all the filaments appear to have dissolved but there may still be large molecular chains present which do not show up on OM. A series of filaments were spun, using BC solutions after dissolving 10, 12, 14, 16 and 18 h and it can be seen from Fig. 4 that the RBC/BC filaments both in dry state and wet state exhibit similar trends in that the breaking strength and elongation of the filament increases first and then decreases. When the dissolving time is 14 h, the breaking strength and elongation of the filaments reach the maximum values of 6.5 cN/dtex and 7.1% respectively for RBC/BC filament in the dry state, 4.3 cN/dtex and 14.3% respectively for RBC/BC filament in wet state, signifying that both the wet and dry RBC/BC filaments have a very high mechanical performance. After 14 h stirring time the breaking strength and elongation of the filaments decreases after this period. By contrast, the standard deviations decrease with the increase of dissolving time reflecting relatively more uniform internal structure and good stability of fibers.

Fig. 4

Therefore, the mechanical properties of RBC filaments depend on the dissolving time and the BC can be considered completely dissolved after 18 h. However, since the best mechanical performance was obtained after 14 h the corresponding filaments were used in all further experiments. The reason for the strength enhancement may be due to the ultra-fine structure existing in the undissolved BC as discussed above.

3.3. Rheological behavior of the BC/DMAc/LiCl mixed solvent

Rheological behavior can be used to give an indication of the potential uses of a polymeric material and the recorded data (Fig. 5a) shows plots of η_a against $\dot{\gamma}$ of the BC solution at 25 ℃ ($\dot{\gamma}$ is the shear rate and η_a is the apparent viscosity) and indicates that the viscosity of the solution decreases with the increase of shear rate, which shows typical shear thinning.

Fig. 5

In Fig. 5b, the curve is divided into three sections for better analysis and Eq. (1) was calculated from the test results. The curve in the low shear rate region shows that the non-Newtonian index (n) of the BC solution at 25 ℃ is 0.9055 but as the shear rate increases and the curve becomes concave and the slope decreases. At the third stage, in the high shear rate region, the data indicates the non-Newtonian index (n) dropped to 0.4778, which being much less than 1.0 suggests that the RBC spinning dope is a non-Newtonian pseudoplastic fluid, consistent with previous work [20]. Thus, the BC/DMAc/LiCl solution exhibits the requirements for wet spinning.

3.4. Morphology analysis

Fig. 6

It can be seen that the morphology of BC changes considerably after regeneration where the BC has an integrated 3-D nanofiber network structure (Fig. 6a) while RBC film (Fig. 6b) has a dense structure since no porosity was

observed even at a magnification of 10 000x. Fig. 6c and 6d show the RBC filaments, without and with stretching, and both have obvious groove structures with a diameter of 50~60 μm possibly caused by the low solid content of the spinning solution and interestingly, the groove structure after stretching was much more uniform. Fig. 6e and 6f will be discussed in section (3.7 Enzymatic hydrolysis).

3.5. XRD analysis

Fig. 7

XRD measurements were conducted on the BC nanofibers and RBC/BC microfilaments and the diffractograms, shown in Fig. 7, indicate that significant changes have occurred in the crystal form of BC after regeneration. Three strong Bragg peaks at 2θ = 14.46°, 16. 85° and 22.62° which are indexed as the (100), (010) and (110) peaks of the typical cellulose Iα form are observed, while the RBC/BC filament shows only two strong main peaks at about 2θ = 12.58° and 20.40°. The peak at 12.58° represents (010) reflection, and actually, the peak at about 20.40° comprises the (100), (012) and (1-10) reflections with very strong contributions from (100) and (1-10). This is consistent with the peaks of the cellulose III_I crystal form with preferred orientation due to the stretching procedure during wet spinning. It should be noted that the analysis of these results are based on the study of French [30].

Moreover, the degree of crystallinity was calculated from the X-ray diffractometer data (also shown in Fig. 7) and it is clearly seen that the degree of crystallinity of BC is 60.29%, while that of the RBC/BC filaments has decreased considerably to 33.22% perhaps due to crystallite growth after regeneration was incomplete. These results indicate that the transformation from cellulose Iα to cellulose III_I occurred after the remodeling of BC and suffered a severe

decline on the degree of crystallinity. It can be also noticed that the typical peaks of BC were not found, probably because of the low BC content.

3.6. FTIR spectroscopy

The BC nanofiber membranes and RBC/BC microfilaments were characterized by FTIR (Fig. 8) performed in order to elucidate whether the characteristic groups of BC have changed after regeneration. The absorption at 3385 cm^{-1} is due to the stretching vibration of –OH groups, including $–CH_2–OH$ and –CH–OH, and the band at 2900 cm^{-1} corresponds to aliphatic –C–H groups and the absorption band for C–H symmetric bending is seen around 1417 cm^{-1}. Additionally, a sharp peak at 1060 cm^{-1} reflects the skeletal vibration of the C–O–C pyranose ring. Thus, for both BC and RBC/BC, the identical characteristic peaks at 3385, 2920, 1630, 1417 and 1060 cm^{-1} can be easily found in the spectra. However, there are apparent differences fingerprint region between 1350~650 cm^{-1} which may be caused by the absorption intensity of the characteristic band or the variation of crystal forms. Overall, these results indicate that no chemical changes had occurred during the dissolution and coagulation processes [20,31].

Fig. 8

3.7. Enzymatic hydrolysis

The DNS method [16] is used to determine the degree of enzyme degradation [31]. The hydrolysis profiles of the BC slurry and the RBC/BC filaments using hydrolysis methods (1) and (2) (see section 2.10 above) are shown in Fig. 9a and 9b respectively and it can be seen that the rate of hydrolysis of the RBC/BC filaments is faster than the BC slurry in both methods.

Fig. 9

Fig. 9a shows that the amount of reducing sugar (RSA) produced from the RBC filaments is always higher than from the BC slurry under every cellulase concentration. The RSA for the RBC/BC filaments was 85 mg while BC slurry produced 60 mg when the cellulase concentration was 50 mg/mL. Similar results were found (Fig. 9b) when both samples were subjected to hydrolysis over the same time (84 h) and in this instance the RBC/BC gave 62 mg and the BC slurry 37 mg respectively.

A number of factors, such as degree of polymerization (DP), crystallinity, accessible surface area and specific surface area are known to affect hydrolysis [32]. As discussed above, the characteristics of BC including polymerization (DP), crystallinity and accessible surface area have changed dramatically after regeneration and as the DP and crystallinity decreased, the accessible surface area increased. Hence, it is reasonable that the RSA of BC is greater than RBC/BC under the same conditions and consequently it can be inferred that the RBC/BC material is more easily degraded than the BC. Moreover, the morphology of the RBC/BC filament after enzymatic hydrolysis for 48 and 84 h, shown in Fig. 6e and 6f, has changed dramatically due to partial degradation.

3.8. Detection of residual solvent

As residual solvents (RS) and residual ions (RI) may represent a potential risk for human health due to their toxicity and their undesirable side effects [33], an attempt was made to detect residuals, especially lithium ions in the RBC/BC filaments. It has been reported that lithium can either inhibit or stimulate growth of normal [34,35] and cancer cells [36,37] and has dose-dependent effects [38]. Lithium has a narrow therapeutic index, with therapeutic

levels between 0.6 and 1.5 mEq/L [38,39] and because toxicity can occur at levels of >1.5 mEq/L, lithium levels must be carefully monitored.. Thus, ICP detection (of Li ions) and GC-MS analysis (DMAc) were used to evaluate the amount of the residuals in the RBC/BC filaments and this information provides novel, significant, data.

3.8.1. ICP determination of the lithium ion concentration

ICP detection was used to determine the concentration of lithium ions (Li^+) present [28,40] and the amounts found in the RBC filament with and without post-treatment are 0.07 and 9.17 mg/g (w/w) respectively. Hence, this study indicated that there is a very small amount of residual Li^+ in the RBC filament after treatment indicating that the post-treatment process is very important for removing lithium from the RBC filaments.

3.8.2. GC-MS detection of DMAc concentration

Fig. 10

In the current work, a headspace gas chromatographic (HSGC) method was used for the determination of residual DMAc in the RBC/BC filaments and Fig. 10 shows the decrease in peak areas, of DMAc in filament samples: (S_1) after pre-stretching bath, (S_2) after sec-stretching bath and (S_3) after post-treating process. According to the standard curve of DMAc in acetone and its fitting formula (Y = 541741 X – 33861) the RBC/BC filaments still contained a low amount of DMAc (46.04 µg/g) after pre-stretching bath and this decreased to 18.21 µg/g after the sec-stretching bath and after post-treatment the content of DMAc further decreased to 8.51 µg/g This process improved the biocompatibility of the RBC/BC filaments showing that the post-treatment is an effective way to reduce RS.

3.9. Evaluation of *In Vitro* Cytocompatibility

For a biomaterial, it is important to evaluate cytocompatibility and several previous studies have indicated that BC has good biocompatibility [41-43]. In this work, *in vitro* tests were performed on BC fragments and RBC/BC filaments respectively, and the results are shown in Fig. 11 and Fig. 12. After incubation for 1, 3 and 5 days, the L929 cells proliferated on different materials displayed significant dissimilarities (Fig. 11). Except for the filaments without post-treatment, the cells on all other samples showed good proliferative results with increasing culture time. It is obvious that apoptosis became more serious with the increase of culture time for the sample without post-treatment. It can be preliminarily concluded that the residuals in the RBC/BC filament without post-treatment will lead to cell apoptosis.

Fig. 11

Fig. 12

It is clearly evident (Fig. 12) that after incubation for 1, 3 and 5 days, the MTT absorbance of control, filaments with post-treatment and native BC fragments all enhanced with the increase of culture time. However, for the sample without post-treatment, the MTT value increased slightly after 3 days of culture and then decreased on the fifth day which is consistent with Fig. 11. Further, compared with the filaments with post-treatment and native BC fragments, the MTT absorbance of the former was higher. The reason could be that the specific surface area of the filaments is relatively large, more suitable for cell adhesion and proliferation, and the release amount of lithium is so low that it does not inhibit the proliferation of L929 cells. Hence, it is necessary to remove the residuals in the RBC/BC fibers

when using DMAc/LiCl as solvent. After removal of residual materials the RBC/BC filaments can promote adhesion and proliferation of L929 cells and can be used as biomaterials.

4. Conclusions

In this work, a structure consisting of a more hyperfine and oriented nanofibril bundle of BC has been prepared and shows high mechanical strength. A novel strategy of partially dissolving the BC was used and this vastly enhanced the mechanical performance of the resulting spun RBC/BC filament. The RBC/BC filament both in the dry state and wet state had the best mechanical performance when the dissolving time was 14 h. After dissolution and remodeling of the BC, the crystal form was transformed from cellulose Iα to cellulose III_I and the degree of crystallinity of RBC/BC was much lower than the original BC. The RBC/BC material was more easily degraded enzymatically than BC due to decreased DP and crystallinity and increased accessible surface area. For the first time, ICP detection and GC-MS analysis were used for evaluating the amount of Li^+ and residual solvent (DMAc) in the RBC/BC filament and it was found that final filament product had a very low content of Li^+ and DMAc and, using L929 cells in *in-vitro* cytocompatibility testing, no cytotoxicity was found for the final RBC/BC filaments. This study provides reference data to aid the development of biomedical and tissue engineering materials with high mechanical strength with potential for further application as a biomaterial

Acknowledgments

This investigation was supported by the grant 16410723700 from the Science and Technology Commission of Shanghai Municipality, the Biomedical Textile Materials "111 Project" of the Ministry of Education of China (No. B07024), the UK-China Joint Laboratory for Therapeutic Textiles (based at Donghua University), and the Yancheng Institute of Industry Technology.

References

[1] H.-P. Fink, J. Ganster, A. Lehmann, Progress in cellulose shaping: 20 years industrial case studies at Fraunhofer IAP, Cellulose, 21 (2014) 31-51.

[2] W. Tang, S. Jia, Y. Jia, H. Yang, The influence of fermentation conditions and post-treatment methods on porosity of bacterial cellulose membrane, World J. Microbiol. Biotechnol., 26 (2010) 125-131.

[3] C. Chen, T. Zhang, Q. Zhang, X. Chen, C. Zhu, Y. Xu, J. Yang, J. Liu, D. Sun, Biointerface by Cell Growth on Graphene Oxide Doped Bacterial Cellulose/Poly (3, 4-ethylenedioxythiophene) Nanofibers, ACS Appl. Mater. Interfaces, 8 (2016) 10183-10192.

[4] J. Kim, Z. Cai, Y. Chen, Biocompatible bacterial cellulose composites for biomedical application, J. Nanotechnol. Eng. Med., 1 (2010) 011006.

[5] S. Kirdponpattara, A. Khamkeaw, N. Sanchavanakit, P. Pavasant, M. Phisalaphong, Structural modification and characterization of bacterial cellulose-alginate composite scaffolds for tissue engineering, Carbohydr. Polym., 132 (2015) 146-155.

[6] A. Meftahi, R. Khajavi, A. Rashidi, M. Sattari, M. Yazdanshenas, M. Torabi, The effects of cotton gauze coating

with microbial cellulose, Cellulose, 17 (2010) 199-204.

[7] T. Zhang, W. Wang, D. Zhang, X. Zhang, Y. Ma, Y. Zhou, L. Qi, Biotemplated synthesis of gold nanoparticle–bacteria cellulose nanofiber nanocomposites and their application in biosensing, Adv. Funct. Mater., 20 (2010) 1152-1160.

[8] N. Jia, S.-M. Li, M.-G. Ma, J.-F. Zhu, R.-C. Sun, Synthesis and characterization of cellulose-silica composite fiber in ethanol/water mixed solvents, BioResources, 6 (2011) 1186-1195.

[9] M. Phisalaphong, T. Suwanmajo, P. Sangtherapitikul, Novel nanoporous membranes from regenerated bacterial cellulose, J. Appl. Polym. Sci., 107 (2008) 292-299.

[10] Q. Yi-min, Comparative study of the properties of alginate and chitosan fibers, J. Text. Res., 1 (2006) 031.

[11] M.F. Güleçyüz, A. Mazur, C. Schröder, C. Braun, A. Ficklscherer, B.P. Roßbach, P.E. Müller, M.F. Pietschmann, Influence of Temperature on the Biomechanical Stability of Titanium, PEEK, Poly-L-Lactic Acid, and β–Tricalcium Phosphate Poly-L-Lactic Acid Suture Anchors Tested on Human Humeri In Vitro in a Wet Environment, Arthroscopy., 31 (2015) 1134-1141.

[12] H.-l. Wu, D.H. Bremner, H.-y. Li, Q.-q. Shi, J.-z. Wu, R.-q. Xiao, L.-m. Zhu, A novel multifunctional biomedical material based on polyacrylonitrile: Preparation and characterization, Mater. Sci. Eng., C, 62 (2016) 702-709.

[13] X. Huang, Fabrication and Properties of Carbon Fibers, Materials, 2 (2009) 2369-2403.

[14] Q. Gao, X. Shen, X. Lu, Regenerated bacterial cellulose fibers prepared by the NMMO· H_2O process, Carbohydr. Polym., 83 (2011) 1253-1256.

[15] G. Shanshan, W. Jianqing, J. Zhengwei, Preparation of cellulose films from solution of bacterial cellulose in

NMMO, Carbohydr. Polym., 87 (2012) 1020-1025.

[16] H. Zhao, C.L. Jones, G.A. Baker, S. Xia, O. Olubajo, V.N. Person, Regenerating cellulose from ionic liquids for an accelerated enzymatic hydrolysis, J. Biotechnol., 139 (2009) 47-54.

[17] S.J. Haward, V. Sharma, C.P. Butts, G.H. Mckinley, S.S. Rahatekar, Shear and extensional rheology of cellulose/ionic liquid solutions, Biomacromolecules, 13 (2012) 1688-1699.

[18] P. Chen, H.-S. Kim, S.-M. Kwon, Y.S. Yun, H.-J. Jin, Regenerated bacterial cellulose/multi-walled carbon nanotubes composite fibers prepared by wet-spinning, Curr. Appl. Phys., 9 (2009) e96-e99.

[19] S.-M. Li, N. Jia, J.-F. Zhu, M.-G. Ma, R.-C. Sun, Synthesis of cellulose–calcium silicate nanocomposites in ethanol/water mixed solvents and their characterization, Carbohydr. Polym., 80 (2010) 270-275.

[20] X. Lu, X. Shen, Solubility of bacteria cellulose in zinc chloride aqueous solutions, Carbohydr. Polym., 86 (2011) 239-244.

[21] Y. Li, H. Jiang, W. Zheng, N. Gong, L. Chen, X. Jiang, G. Yang, Bacterial cellulose–hyaluronan nanocomposite biomaterials as wound dressings for severe skin injury repair, J. Mater. Chem. B, 3 (2015) 3498-3507.

[22] X. Liu, P.X. Ma, Polymeric scaffolds for bone tissue engineering, Ann. Biomed. Eng., 32 (2004) 477-486.

[23] C.M. Teglia, M. Montemurro, M.M. De Zan, M.S. Cámara, Multiple responses optimization in the development of a headspace gas chromatography method for the determination of residual solvents in pharmaceuticals, J. Pharm. Anal., 5 (2015) 296-306.

[24] X. Yang, E.D. Cranston, Chemically Cross-Linked Cellulose Nanocrystal Aerogels with Shape Recovery and Superabsorbent Properties, Chem. Mater., 26 (2014) 6016-6025.

[25] Y. Habibi, L.A. Lucia, O.J. Rojas, Cellulose Nanocrystals: Chemistry, Self-Assembly, and Applications, Chem.

Rev., 110 (2010) 3479.

[26] T.K. Ghose, Measurement of cellulase activities, Pure Appl. Chem., 59 (1987) 257-268.

[27] G.L. Miller, Use of dinitrosalicylic acid reagent for determination of reducing sugar, Anal. Chem., 31 (1959) 426-428.

[28] J. Obradovic, H. Wondraczek, P. Fardim, L. Lassila, P. Navard, Preparation of three-dimensional cellulose objects previously swollen in a DMAc/LiCl solvent system, Cellulose, 21 (2014) 4029-4038.

[29] G.I. Mantanis, R.A. Young, R.M. Rowell, Swelling of compressed cellulose fiber webs in organic liquids, Cellulose, 2 (1995) 1-22.

[30] A.D. French, Idealized powder diffraction patterns for cellulose polymorphs, Cellulose, 21 (2014) 885-896.

[31] A.M. de Araújo Júnior, G. Braido, S. Saska, H.S. Barud, L.P. Franchi, R.M. Assunção, R.M. Scarel-Caminaga, T.S. Capote, Y. Messaddeq, S.J. Ribeiro, Regenerated cellulose scaffolds: preparation, characterization and toxicological evaluation, Carbohydr. Polym., 136 (2016) 892-898.

[32] R.P. Chandra, R. Bura, W.E. Mabee, A. Berlin, X. Pan, J.N. Saddler, Substrate Pretreatment: The Key to Effective Enzymatic Hydrolysis of Lignocellulosics?, Adv. Biochem. Eng. Biotechnol., 108 (2007) 67-93.

[33] C.M. Teglia, M. Montemurro, M.M.D. Zan, M.S. Cámara, Multiple responses optimization in the development of a headspace gas chromatography method for the determination of residual solvents in pharmaceuticals, J. Pharm. Anal., 5 (2015) 296-306.

[34] J.C. Laurenz, S.B. Smith, Lithium chloride does not inhibit the proliferation of L6 myoblasts by decreasing intracellular free inositol, J. Anim. Sci., 76 (1998) 66-73.

[35] A.J. Polotsky, L. Zhu, N. Santoro, J.W. Pollard, Lithium chloride treatment induces epithelial cell proliferation

in xenografted human endometrium, Hum. Reprod., 24 (2009) 1960-1967.

[36] S. Ayla, A. Bilir, B.C. Soner, O. Yilmazdilsiz, M. Ergüven, G. Oktem, Notch signaling-related therapeutic strategies with novel drugs in neuroblastoma spheroids, J. Pediatr. Hematol. Oncol., 36 (2012) 37-44.

[37] T.R. O'Donovan, S. Rajendran, S. O'Reilly, G.C. O'Sullivan, S.L. Mckenna, Lithium Modulates Autophagy in Esophageal and Colorectal Cancer Cells and Enhances the Efficacy of Therapeutic Agents In Vitro and In Vivo, Plos One, 10 (2015).

[38] M. Suganthi, G. Sangeetha, G. Gayathri, B.R. Sankar, Biphasic Dose-Dependent Effect of Lithium Chloride on Survival of Human Hormone-Dependent Breast Cancer Cells (MCF-7), Biol. Trace Elem. Res., 150 (2012) 477-486.

[39] M.D. Okusa, L.J. Crystal, Clinical manifestations and management of acute lithium intoxication, Am. J. Med., 97 (1994) 383-389.

[40] R. Sczech, H. Riegler, Molecularly smooth cellulose surfaces for adhesion studies, J. Colloid Interface Sci., 301 (2006) 376-385.

[41] C. Zhu, F. Li, X. Zhou, L. Lin, T. Zhang, Kombucha‐synthesized bacterial cellulose: Preparation, characterization, and biocompatibility evaluation, J. Biomed. Mater. Res., Part A, 102 (2014) 1548-1557.

[42] D.O.S. Recouvreux, C.R. Rambo, F.V. Berti, C.A. Carminatti, R.V. Antônio, L.M. Porto, Novel three-dimensional cocoon-like hydrogels for soft tissue regeneration, Mater. Sci. Eng., C, 31 (2011) 151-157.

[43] Y. Hu, J.M. Catchmark, E.A. Vogler, Factors Impacting the Formation of Sphere-Like Bacterial Cellulose Particles and Their Biocompatibility for Human Osteoblast Growth, Biomacromolecules, 14 (2013) 3444-3452.

Fig. 1

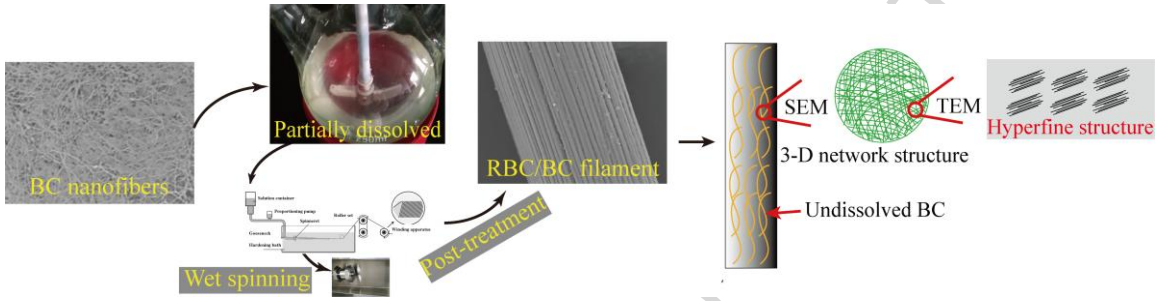

Fig. 1. The preparation strategy of strength enhanced RBC/BC microfilaments: Morphology transition from original BC nanofibers to RBC/BC microfilament.

Fig. 2

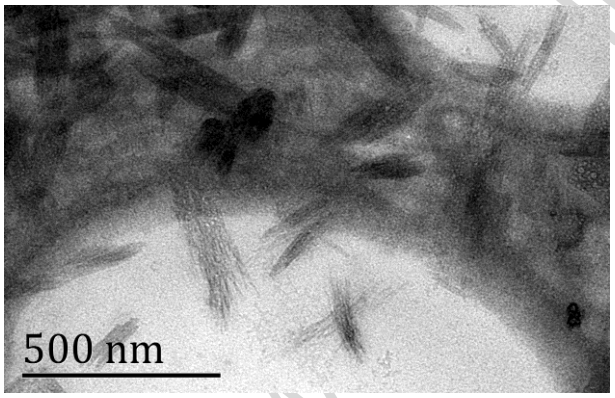

Fig. 2. TEM image of the acid-hydrolysis products of BC.

Fig. 3

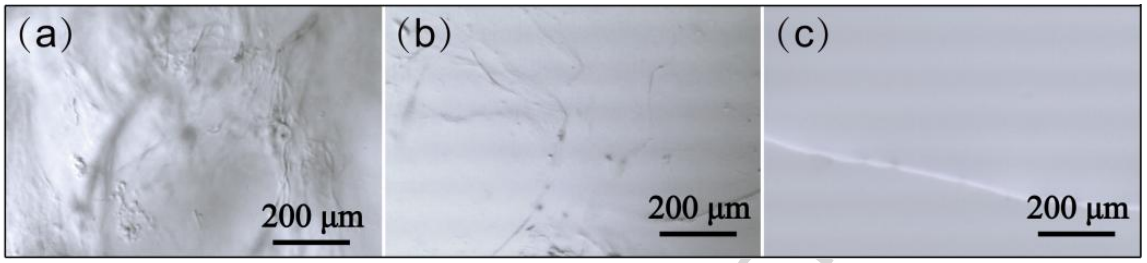

Fig. 3. Optical micrographs during the swelling process of BC in the DMAc/LiCl solvent system: (a) 6 h; (b) 10 h and (c) 14 h.

Fig. 4

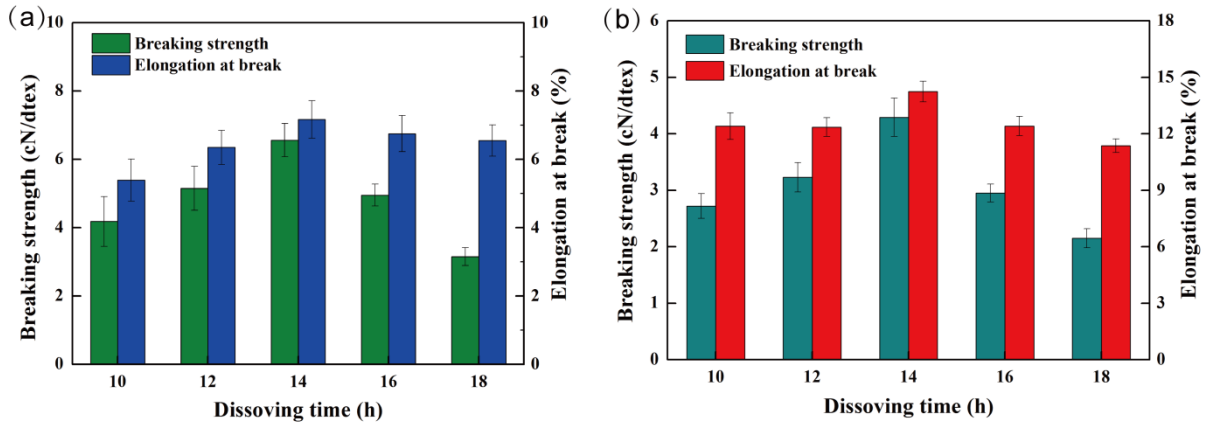

Fig. 4. Mechanical parameters of the RBC/BC filaments for (a) in dry state and (b) in wet state.

Fig. 5

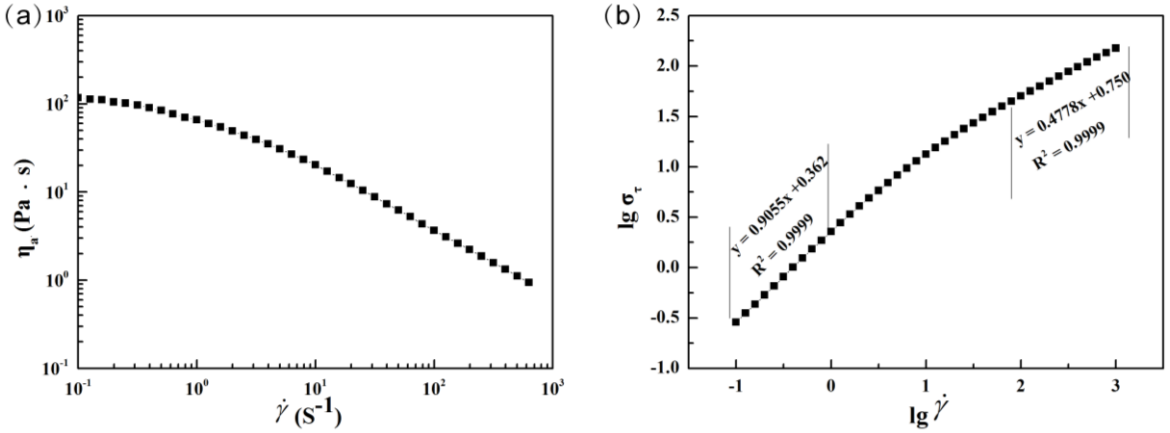

Fig. 5. Rheological behavior of 2% BC/DMAc/LiCl solution at 25 ℃ of (a) flow curves and (b) non-Newtonian index n.

Fig. 6

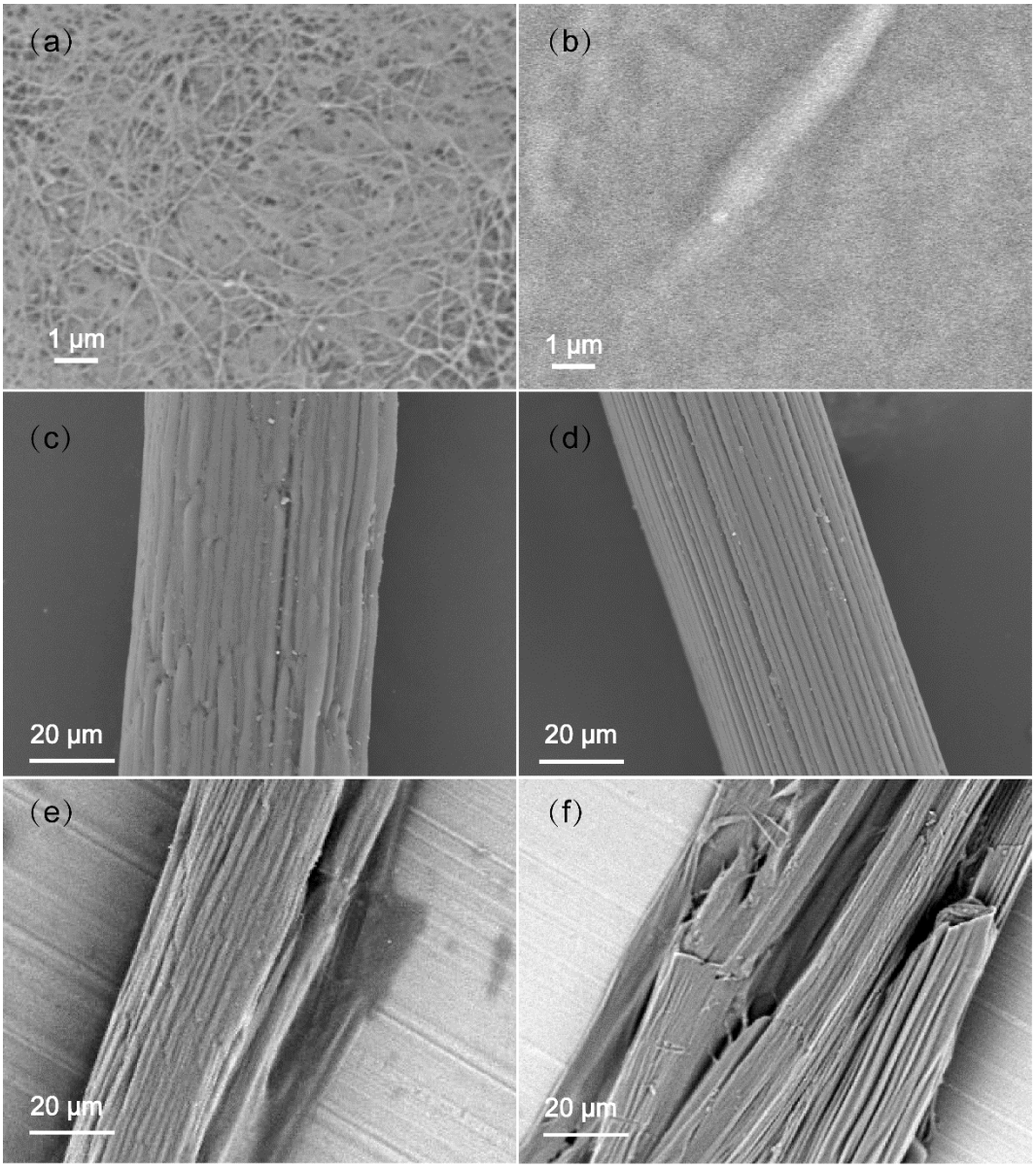

Fig. 6. SEM images of the surface morphology of the (a) original BC nanofibers membrane (10000×); (b) recast RBC film (10000×); (c) RBC microfilaments without stretching (1000×); (d) RBC microfilaments after stretching; (e) RBC microfilaments degraded for 48 h (1000×); and (f) RBC microfilaments degraded for 84 h (1000×).

Fig. 7

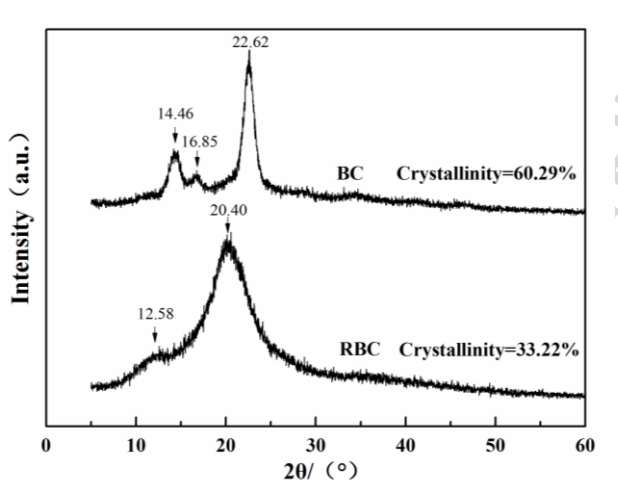

Fig. 7. X-Ray diffractogram of BC nanofibers and RBC microfilaments.

Fig. 8

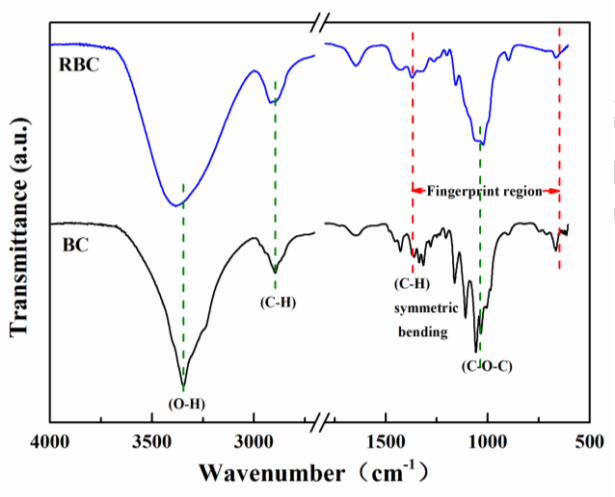

Fig. 8. FTIR spectra of the BC nanofibers and RBC/BC microfilaments.

Fig. 9

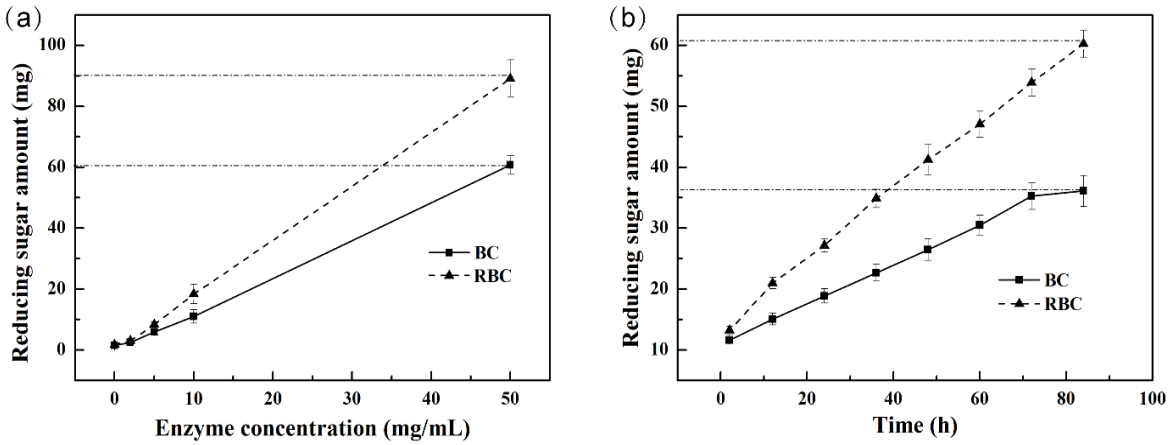

Fig. 9. Enzymatic hydrolysis of nanofibers and RBC microfilaments using (a) method (1) and (b) method (2).

Fig. 10

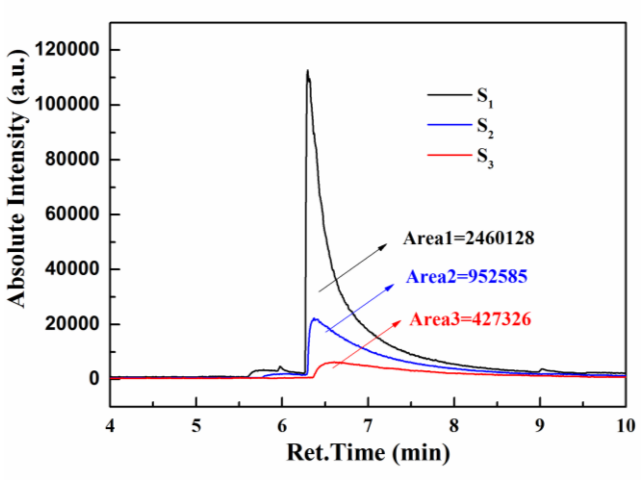

Fig. 10. GC-MS chromatogram of residual DMAc in the filament samples: (S_1) after pre-stretching bath;(S_2) after sec-stretching bath; and (S_3) after post-treatment process.

Fig. 11

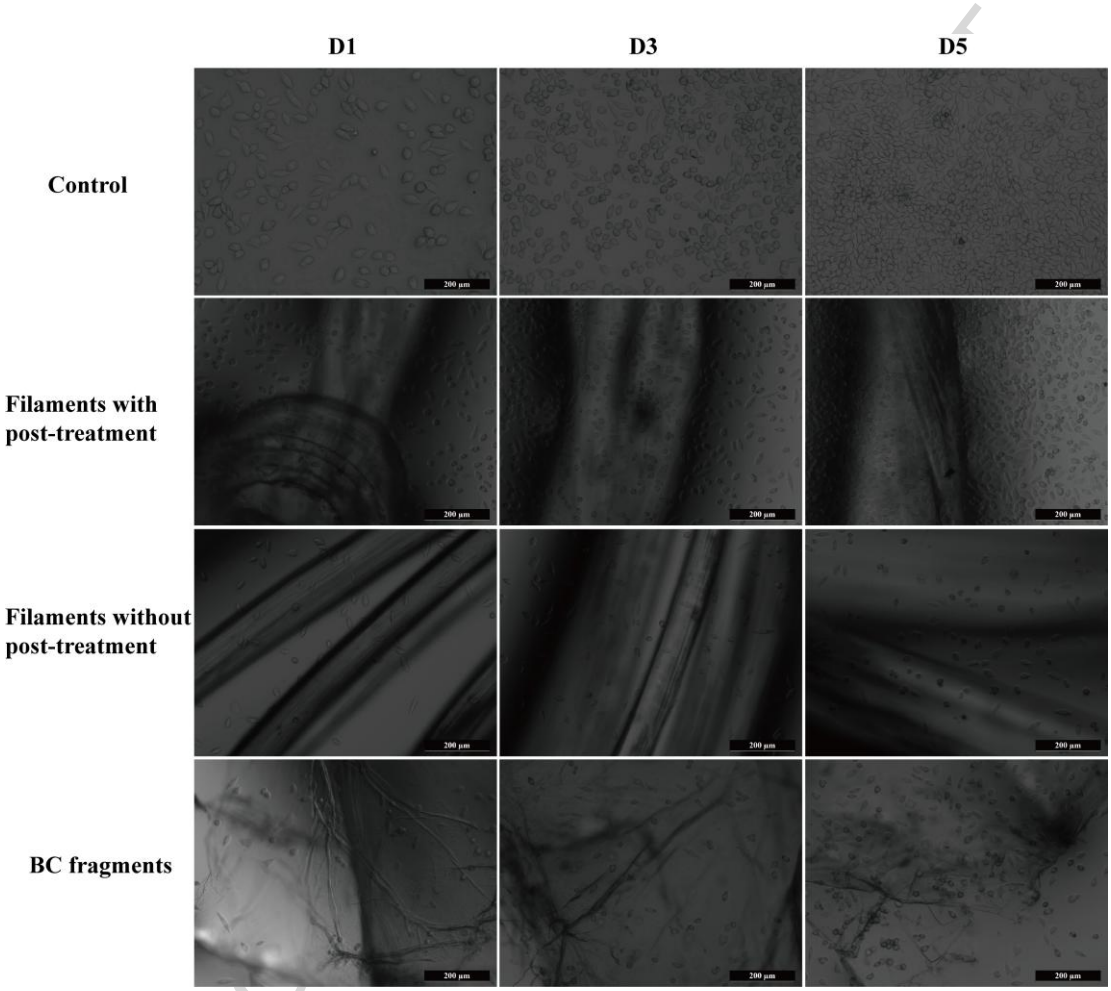

Fig. 11. Microscopic images of L929 cells proliferated on different materials. The scale bar in each panel represents 200 µm.

Fig. 12

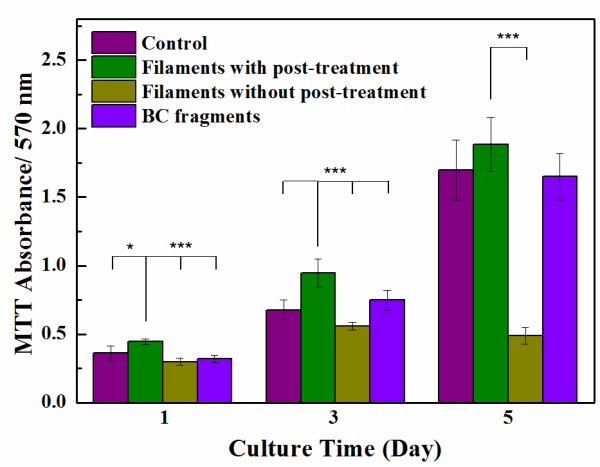

Fig. 12. MTT Cell viability of the L929 cells on different materials. Data are reported as mean ± S.D. from six independent experiments. Data are annotated with * for $p < 0.05$, ** for $p < 0.01$, and *** for $p < 0.001$ which were used to evaluate the significance of the experimental data.

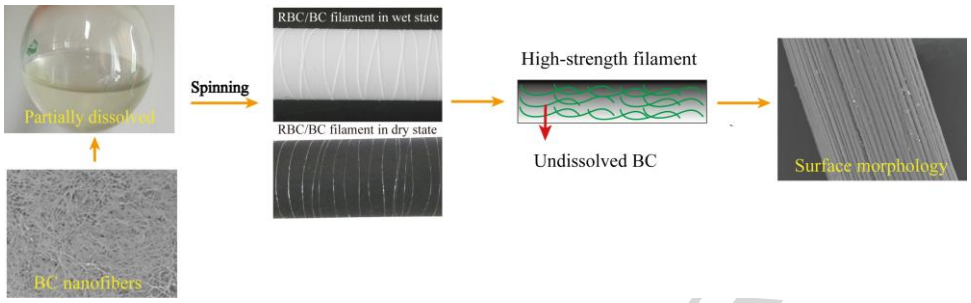

Graphical abstract

Highlights

1 Bacterial cellulose nanocrystals (BCNCs) with a highly oriented nanofibril bundle structure have been prepared and investigated.

2 The structure of the BCNCs indicates that bacterial cellulose (BC) has a secondary hyperfine structure consisting of nanofibrils with diameters of just several nanometers.

3 A novel strategy involving partial dissolution BC greatly enhanced the mechanical performance of the spun filaments.

4 An effective post-treatment process was utilized to remove residual solvents from the RBC/BC microfilaments to ensure biocompatibility.